Nanoscale

Enabling Practical Nanoparticle Electrodeposition from Aqueous Nanodroplets

Journal:	*Nanoscale*
Manuscript ID	NR-ART-12-2021-008045.R1
Article Type:	Paper
Date Submitted by the Author:	07-Jan-2022
Complete List of Authors:	Reyes-Morales, Joshua; The University of North Carolina at Chapel Hill, Chemistry Vanderkwaak, Benjamin; The University of North Carolina at Chapel Hill, Chemistry Dick, Jeffrey; The University of North Carolina at Chapel Hill, Chemistry

Enabling Practical Nanoparticle Electrodeposition from Aqueous Nanodroplets

Joshua Reyes-Morales[a], Benjamin Theodore Vanderkwaak[b], and Jeffrey E. Dick[a,c]*

*Corresponding author: jedick@email.unc.edu

[a] Department of Chemistry, The University of North Carolina at Chapel Hill, Chapel Hill, NC 27599, USA

[b] Department of Biology, The University of North Carolina at Chapel Hill, Chapel Hill, NC 27599, USA

[c] Lineberger Comprehensive Cancer Center, School of Medicine, The University of North Carolina at Chapel Hill, Chapel Hill, NC 27599, USA

Abstract: The rapid rise of technology in the modern world has led to an increased demand for energy. Consequently, it is essential to increase the efficiency of current energy-producing systems due to the poor activity of their catalysts. Nanoparticles play a significant role in energy storage and conversion; however, electrodeposition of nanoparticles is difficult to achieve due to surface heterogeneities, nanoparticle diffusion layer overlap, and the inability to electrodeposit multi-metallic nanoparticles with stoichiometric control. These problems can be solved through nanodroplet-mediated electrodeposition, a technique where water nanodroplets are filled with metal salt precursors that form stable nanoparticles when they collide with a negatively-biased electrode. Further, this method has demonstrated control over nanoparticle size and morphology, displaying a wide variety of applications for the generation of materials with excellent catalytic properties. Historically, the cost of nanodroplet-mediated electrodeposition experimentation is prohibitive because practitioners use 0.1 M to 0.5 M tetrabutylammonium perchlorate (TBAP) dissolved in the oil phase (~10 mL). Such high concentrations of electrolytes have been used to lower ohmic drop and provide ions to maintain charge balance during electrodeposition. Here, we show that supporting electrolyte is not necessary for the oil phase. In fact, one can use a suitable salt (such as lithium perchlorate) in the aqueous phase to achieve nanoparticle electrodeposition. This simple change, grounded in an understanding of ion transfer, drives down the cost per experiment by nearly three orders of magnitude, representing a necessary step forward. The proposed approach presents a promising procedure for future cost-effective energy conversion systems.

Keywords: *Ion Transfer, Voltammetry, Electrodeposition, Nanodroplet-mediated electrodeposition, Particles*

Introduction:

In recent years there has been an increased demand for energy due to the advances in modern technology. A multitude of energy-generating techniques such as fuel cells,[1, 2] batteries,[3] solar cells,[4]and more, exist to satisfy energy demands. Significant applications for harnessed energy include transportation, electric utility, bioenergy processes, etc.[1] These systems rely upon the conversion of chemical energy, from chemical reactions at a conductive material, into electrical energy. To drive this conversion, different materials with varying activities are necessary.[5-8] However, generating the required amount of energy to satisfy the energy demand requires the use of materials that will minimize the input of energy, and maximize the subsequent output. Thus, catalysts, materials that lower activation energy, are necessary to drive reactions in the conversion of chemical energy to electrical energy.[9-11] A common catalyst for the oxygen reduction reaction in fuel cells is platinum. This metal is known to be the best catalyst for the oxygen reduction reaction, as it does not get oxidized at room temperature in the presence of oxygen, has high heat resistance, and high corrosion resistant.[12] There are a myriad of ways to synthesize nanoparticles, such as chemical synthesis,[13] annealing process,[14] bulk electrodeposition,[15] etc. However, since catalysis reactions depend on the size and morphology of the catalyst, most methods require the addition of reducing agents to reduce the average size of the nanoparticles.[16]

A way to control nanoparticle size is through the synthesis in a reverse emulsion system, containing water nanodroplets suspended in an oil phase. Upon the addition of the metal salt precursor in the water droplets with a reducing agent, nanoparticles are formed.[13] Nonetheless, the use of a reducing agent can introduce impurities to the sample.[17] Furthermore, such nanoparticles are generally stabilized by ligands (e.g., citrate) that have an effect on the electrocatalytic properties of the metal nanoparticles formed.[18-21] Direct electrodeposition of nanoparticles allays the aforementioned issues. Classical electrodeposition of nanoparticles suffers from heterogeneities in nanoparticle size and coverage because when nanoparticles form, they compete for precursor salt when their diffusion layers overlap. To mitigate these problems, our group developed nanodroplet-mediated electrodeposition.[22] This procedure is similar to the reverse emulsion synthesis of nanoparticles, however, an electrode is used as the 'reducing agent.'[23-27] This technique provides an array of advantages, such as enabling studies of single nanoparticle growth kinetics, interfacial electron and ion transfer mechanisms,[28] and the electrodeposition of

high entropy alloy nanoparticles[29]. Ahn and co-workers extended this method to not only the deposition of oxyhydroxide nanoparticles[30] and surfactant-free copper nanoparticles,[31] but also polymer nanoparticles.[32] Further, Tschulik and co-workers broadened the approach to the study of electrocatalytic reactions at very small nanoparticles. Our group expanded the use of nanodroplet-mediated electrodeposition to synthesize electrochemically high entropy alloy nanoparticles along with several fundamental studies regarding growth kinetics of single nanoparticles,[33, 34] ion transfer mechanisms in small droplets, and reactivity at the three-phase boundary.[35-37]

One of the greatest drawbacks of electrodeposition from water nanodroplets is that electroneutrality must be satisfied. For instance, the reduction of chloroplatinic acid liberates six chloride anions; to maintain electroneutrality, we added 0.1 – 0.5 M tetrabutylammonium perchlorate (TBAP) to the 1,2-dichloroethane phase. Here, we demonstrate that nanoparticles can be electrodeposited from water nanodroplets without the use of TBAP. The electrodeposition consists of the addition of hexachloroplatinic acid with lithium perchlorate ($LiClO_4$) in the water droplets suspended in the 1,2-dichloroethane phase. When water droplets collide with a conductive substrate at a potential biased enough to facilitate the electron transfer from the solid phase to the redox molecules in the water droplets, $PtCl_6^{2-}$ is reduced to form zero-valent Pt nanoparticles at the electrode surface (**Scheme 1**). In the presence of TBAP in the 1,2-dichloroethane phase (**Scheme 1a**), TBA^+ migrates into the water droplet to maintain the charge balance upon the reduction of $PtCl_6^{2-}$ to Pt^0.[29] In the presence of $LiClO_4$ (**Scheme 1b**), we hypothesize that the perchlorate anion needs to leave the droplet to maintain charge balance. Here, we demonstrate nanoparticle formation and use stochastic electrochemistry to validate the ion transfer hypothesis. Additionally, we show that this new technique is orders of magnitude cheaper than using salt in the organic phase, enabling practical electrodeposition moving forward. This approach offers a promising way of performing future electrochemical experiments such as nanoparticle electrosynthesis and electrochemical studies *via* stochastic collisions in a cost-effective way.

Experimental:

Reagents and Materials

The oil phase, dichloroethane (1,2-DCE, 99.8%), and the supporting electrolyte, tetrabutylammonium perchlorate (99%), were obtained from Sigma-Aldrich. The metal precursor hexachloroplatinic acid was obtained from Sigma-Aldrich as an 8% w/v stock solution. The

supporting electrolyte for the water phase, lithium perchlorate (battery grade, 99.99% trace metals basis), was obtained from Sigma-Aldrich. Potassium ferricyanide (99.98 % trace metals basis) was obtained from Sigma-Aldrich. The gold ultramicroelectrode (Au UME) with 12.5 μm diameter and the glassy carbon macroelectrode (3 mm diameter) were purchased from CH Instruments (Austin, TX). The highly oriented pyrolytic graphite (HOPG) substrate was purchased from Momentive Performance Materials Quartz, Inc. The electrodes were polished using three different polishing clothes containing 1-micron alumina powder (CH Instruments), 0.3-micron alumina powder (CH Instruments), and polishing cloth with water respectively. All water-soluble reagents were dissolved in nano-pure water (18.2 MΩ·cm).

Instrumentation

The water-in-oil emulsions were prepared using a Q500 ultrasonic processor (Qsonica, Newtown, CT) with a 1/16th'' microtip probe using a pulse sonication method of 5 seconds on and 5 seconds off for a total of 6 cycles at 40% amplitude. Electrochemical experiments such as cyclic voltammetry and amperometric *i-t* curve were performed using a CHI model 601D potentiostat (CH Instruments, Austin, TX). The reference electrode was an Ag/AgCl stored in a solution of 1 M KCl and placed into solution *via* a salt bridge. The counter electrode was a glassy carbon rod. The images of the nanoparticles were obtained using Scanning Electron Microscopy (SEM) and Energy Dispersive Spectroscopy (EDS) for element confirmation. Parameters used were: 5 keV, 20 keV and 0.69 nA. The instrument used was a Helios 600 Nanolab dual beam system (FEI, Hillsboro, OR) and INCA PentaFET-x3 (Oxford, Abingdon, UK). NPs were deposited *via* amperometry using a PTFE cell with a 2 mm diameter Viton O-ring where the HOPG had an exposed diameter of 2 mm. The HOPG surfaces were exfoliated between experiments using adhesive tape to take out the layers for exposing a cleaner surface. All electrochemical experiments are presented using the polarographic notation (Texas). All cathodic currents are shown as positive while anodic reaction currents are shown as negative currents. The semi-quantitative analysis of particles in Figure 1h was performed by identifying the nanoparticles that appeared spherical in shape and comparing them to nanoparticles that did not appeal spherical in shape.

Preparation of solutions

Water-in-oil emulsions: 25 μL of a water solution containing different reagents was added to 5 mL of a solution of 1,2-dichloroethane (with and without 0.1 M TBAP). For the

electrodeposition and collision experiments of Pt in the presence of $LiClO_4$, the water droplets contained 50 mM hexachloroplatinic acid with 250 mM $LiClO_4$ suspended in a solution of 1,2-dichloroethane (without TBAP). In the case of the electrodeposition and collision experiments of Pt in the presence of TBAP, the water droplets contained 50 mM hexachloroplatinic acid suspended in 1,2-dichloroethane with 0.1 M TBAP. Amperometric *i-t* curves of potassium ferricyanide in the presence of $LiClO_4$ contained 20 mM potassium ferricyanide with 20 mM $LiClO_4$ in water droplets suspended in 1,2-dichloroethane (without TBAP). In the presence of TBAP, the water droplets only contained 20 mM potassium ferricyanide suspended in 1,2-dichloroethane with 0.1 M TBAP. The solution was prepared in a 10 mL Oak Rids Centrifuge Tube, fluorinated ethylene propylene from Thermo Scientific. The solutions used as controls were prepared as aforementioned but without the redox reagents.

Results and Discussion:

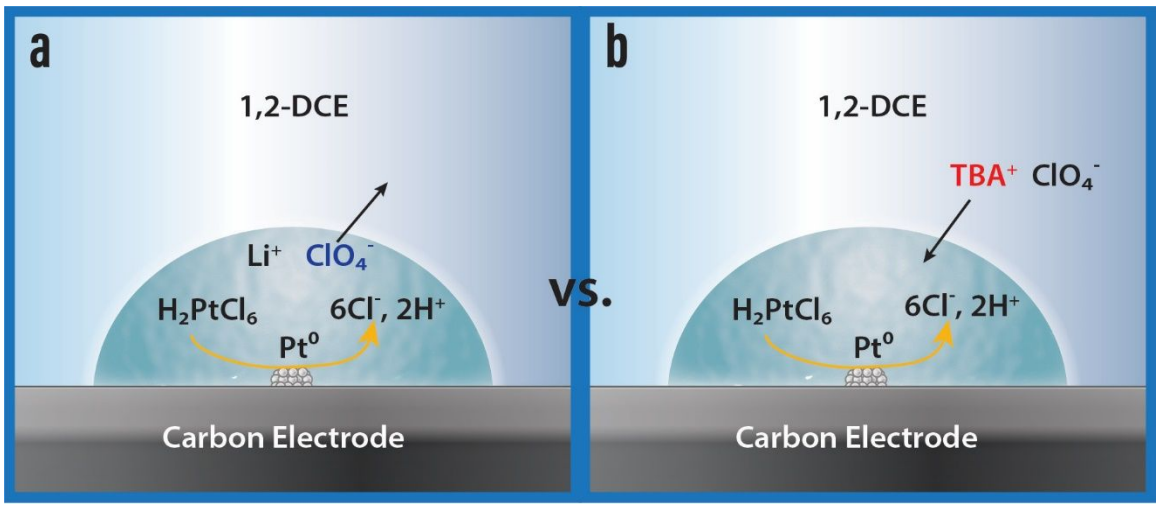

Scheme 1. Representation of single water droplets colliding with the electrode surface. Upon the reduction of $PtCl_6^{2-}$ to Pt^0 by a 4-electron process **a)** in the presence of $LiClO_4$, ClO_4^- should migrate from the droplet to the 1,2-dichloroethane phase to maintain charge balance while **b)** in the presence of TBAP, TBA^+ should migrate from the 1,2-dichloroethane phase into the water droplet**. TBAP= tetrabutylammonium perchlorate**

Electrochemistry in single droplets has been demonstrated to be a useful technique to confine species to deposit nanoparticles, study single entity reactivities, study thermodynamics, and more.[29, 38, 39] This paper presents the electrodeposition of Pt nanoparticles using nanodroplet-

mediated electrodeposition. This method consists of water droplets suspended in the 1,2-dichloroethane phase with the confinement of the metal-salt precursor in the water droplets. Upon the collision of a droplet on the electrode surface at a potential more negative than the standard reduction potential of hexachloroplatinic acid (*e.g.,* 0.504 V vs Ag/AgCl),[40] Pt nanoparticles are generated *via* the electrochemical reduction of $PtCl_6^{2-}$ (**Scheme 1**).[40] It is known that every part of environmental systems maintains equilibrium: such is the same with electrochemical systems. Upon the oxidation or reduction of a species, the system is required to maintain charge neutrality during the electrochemical process to avoid an appreciable electrical field affecting the overall electrochemical process. When Pt cations are reduced to zero-valent Pt, an ion must leave or enter the water droplet to maintain charge balance. Our group has previously deposited Pt nanoparticles using TBAP as the supporting electrolyte in the 1,2-dichloroethane phase (**Scheme 1b**). [29] The Gibbs free energies tell us that is more favorable for TBA^+ to enter the water droplet than for ClO_4^- to leave the water droplet.[35] This suggests that TBA^+ would enter the water droplet to maintain charge balance when Pt cations are being reduced. However, in our present work, we found that it is possible to obtain nanoparticles by adding a small amount of supporting electrolyte in the water droplets, such as $LiClO_4$, without the addition of any supporting electrolyte to the 1,2-dichloroethane phase. In the case of using $LiClO_4$ in the water phase, ClO_4^- will migrate to the oil phase to maintain charge balance (**Scheme 1a**).

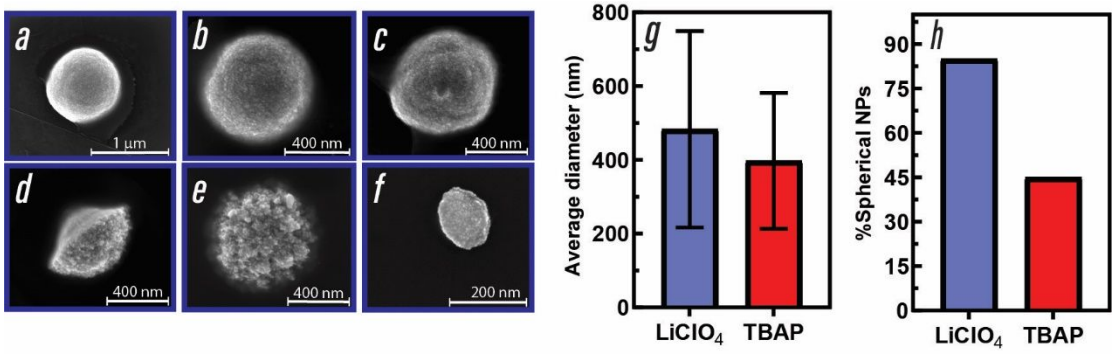

Figure 1. Scanning electron microscopy images of Pt nanoparticles deposited using a water-in-oil emulsion with 50 mM hexachloroplatinic acid in water droplets suspended in 1,2-dichloroethane in the presence of **(a, b, c)** 250 mM $LiClO_4$ in water and **(d, e, f)** 0.1 M TBAP in 1,2-dichloroethane phase. **g)** Graph of assorted sizes and their respective standard deviation is shown. **h)** Graph of percentage of the spherical nanoparticles. The nanoparticles were deposited using amperometry at a biased potential of -0.1 V vs Ag/AgCl for 240 seconds using a highly oriented pyrolytic graphite as the substrate. The number of nanoparticles for the bar graph is N=54 for each set in the presence of $LiClO_4$ or TBAP. See the supporting information file for more information (**S11**). **TBAP= tetrabutylammonium perchlorate**

Within the presented method we obtained electrochemical signals in the presence of $LiClO_4$. Considering that the 1,2-dichloroethane phase does not contain a supporting electrolyte, we hypothesized a high *i*R drop due to Ohm's Law, and that no nanoparticles should be obtained at extremely low overpotentials. Despite that, we found that around –0.1 V vs Ag/AgCl we can still obtain Pt nanoparticles**.** The *i*R drop calculation showed a potential estimation between 9.3 mV to 34 mV (**Figure S1 and S2**), meaning that the potential required to reduce Pt cations is shifted by less than a hundred millivolts, showing that even at -0.1 V vs Ag/AgCl zero-valent Pt nanoparticles can be formed. **Figures 1a-1c** shows representative SEM images of Pt nanoparticles obtained from the system with $LiClO_4$. Even if there is a shift in the potential, at 0.1 V vs Ag/AgCl nanoparticles can be obtained due to the difference between the applied potential and the standard reduction potential of chloroplatinate (e.g., 0.504 V vs. Ag/AgCl).[40] Application of a potential approximately 0.6 V of difference between the applied potential and the standard reduction potential of chloroplatinate represents enough thermodynamic energy applied to reduce $PtCl_6^{2-}$ to zero-valent Pt nanoparticles.[29]

Previously, our group electrodeposited nanoparticles using the nanodroplet-mediated electrodeposition with 0.1 M TBAP in the 1,2-dichloroethane phase.[29] Despite control over the nanoparticle size during electrodeposition, variation in morphology was still observed. **Figures 1d-1f** display representative scanning electron microscopy images of nanoparticles obtained with the electrodeposition of Pt in the presence of TBAP as the supporting electrolyte in the 1,2-dichloroethane phase. When comparing the nanoparticles obtained in the presence of TBAP (**Figures 1d-1f**) versus in the presence of $LiClO_4$ (**Figures 1a-1c**), the morphology is consistent when in the presence of $LiClO_4$. This may be due to the fact that when $LiClO_4$ is in the water phase perchlorate must leave the water droplet to maintain charge balance, minimizing the interferences of ions during the nucleation and growth of the metal nanoparticles. However, when TBAP is included in the 1,2-dichloroethane phase TBA^+ must enter the water droplet and may interact or interfere with the nucleation and growth of the nanoparticles, resulting in their poisoning. Moreover, **Figure 1g** shows the average size and the distribution of the nanoparticles obtained in the presence of TBAP and $LiClO_4$. Since nanodroplet-mediated electrodeposition depends on the stochastic collisions of the water droplets, there is still a large size distribution of the nanoparticles,[29] and more precise control of the size distribution will be a future topic of investigation. Additionally, **Figure 1h** exhibits a bar graph of semi-quantitative measurements of

the percentage of nanoparticles that have a spherical geometry, presenting that around 80% of the nanoparticles have a spherical geometry when they were synthesized in the presence of $LiClO_4$. While in the presence of TBAP, it was observed that only around 45% of the nanoparticles had a spherical geometry. Since $LiClO_4$ is leaving the droplet to maintain charge balance during the reduction of $PtCl_6^{2-}$ to Pt^0, the ions are not interfering with electrodeposition as much compared to the aforementioned methods utilizing TBAP in the oil phase. Several research have shown how different ions are being transferred depending on the potential being applied, which is why we think that the particles morphology differences are due to the ion transfer mechanism.[41, 42]

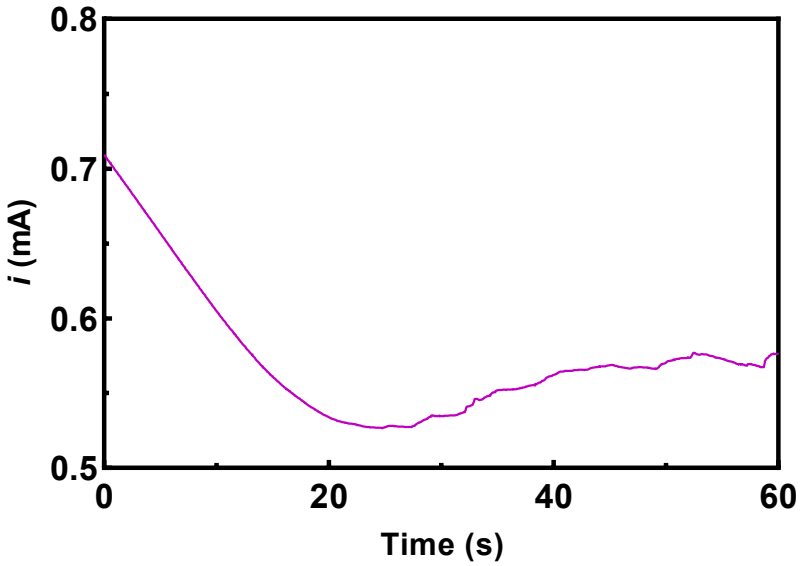

Figure 2. Amperogram of a solution of 50 mM hexachloroplatinic acid with 250 mM $LiClO_4$ in water using a glassy carbon macroelectrode as the working electrode. The applied potential was -0.3 V vs Ag/AgCl.

Despite the high resistance of 1,2-dichloroethane and only containing a supporting electrolyte in the water phase, nanoparticles may still be synthesized *via* electrochemistry. **Figure 2** presents an amperogram of a bulk water solution with 50 mM hexachloroplatinic acid with 250 mM $LiClO_4$. The shape of the amperogram in **Figure 2** can be explained by classical nucleation and growth of a new platinum phase on the carbon electrode.[43] The current begins at a maximum and decays because of double layer relaxation followed by consumption of hexachloroplatinic acid. The current begins to increase again at ~25 s (so-called nucleation induction time[44]) as stable

platinum nuclei form. The current then increases with time because of radial diffusion of hexachloroplatinate to the platinum nuclei and levels off when the diffusion layers of neighboring nuclei begin to overlap. One of the main benefits of using the discussed nanodroplet technique is that diffusion layer overlap of neighboring nanoparticles is not considered because the nanodroplet confines the metal salt precursor. This may be useful in controlling nanoparticle size and morphology and will be the topic of a future investigation. **Figure S10** displays an amperogram of a water-in-oil emulsion with 50 mM hexachloroplatinic acid and 250 mM $LiClO_4$ in water droplets suspended in 1,2-dichloroethane. The observed current-potential trace seems like noise, but this behavior is due to the high resistance of the 1,2-dichloroethane phase (**Figures S1-S2**). Nevertheless, observing a variation in the current response due to the difference in resistance, we hypothesize that if the area of the electrode is small enough, droplets can cover the electrode surface and an electrochemical signal can be observed due to the small charge transfer resistance between the electrode-water interface.

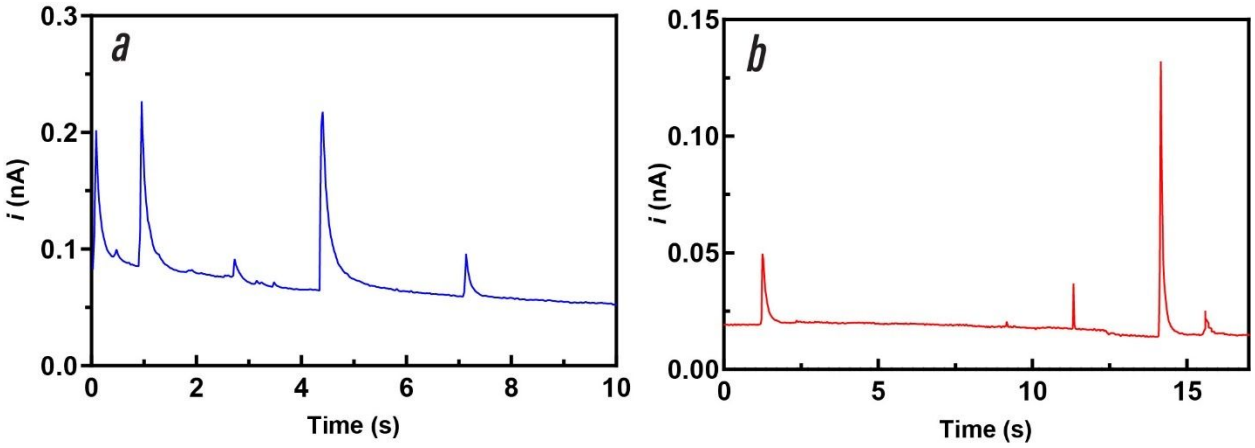

Figure 3. Amperometric *i-t* curves of water droplets containing 20 mM potassium ferricyanide using an Au UME. The first solution contained **a)** 20 mM potassium ferricyanide with 20 mM $LiClO_4$ in water droplets suspended in 1,2-dichloroethane, while the second solution contained **b)** 20 mM potassium ferricyanide in water droplets suspended in 1,2-dichloroethane with 0.1 M TBAP. The average droplet radius for the system with $LiClO_4$ and TBAP is 655 nm ± 209 nm (N=10) and 467 nm ± 134 nm (N=13) respectively. The potential was selected based on the reduction potential of ferricyanide. Applied potential for **Figure 1a** and **1b** was -0.2 vs Ag/AgCl. Droplet sizes were calculated using **Equation 1**. **TBAP= tetrabutylammonium perchlorate**

To illustrate the aforementioned hypothesis, amperometric *i-t* curves were obtained using a well-known redox mediator, potassium ferricyanide, in the presence and absence of $LiClO_4$. A

derivation from Faradays Law allows us to obtain an equation that can be used to determine the size of a single droplet as presented in **Equation 1**.[29]

$$r_{droplet} = \sqrt[3]{\frac{0.75\ Q}{\pi n F C}} \qquad \textbf{Eq. 1}$$

F is the Faraday constant, C is the concentration of hexachloroplatinic acid in the water droplets (e.g., 50 mM), n is the number of electrons transferred (for the reduction of chloroplatinate to zero-valent platinum, 4 e^-), and Q is the charge that is obtained from the integration of the area under the curve of a single collision event in the amperometric *i-t* curve. The differences in the droplet sizes are due to the polydispersity of the droplets in the emulsion, which can vary from emulsion to emulsion.[29]

Figure 3 illustrates the amperometric *i-t* curve of single droplet collisions with 20 mM potassium ferricyanide in the water droplets at -0.2 V vs Ag/AgCl, a potential much more negative than its standard reduction potential of 0.549 V vs. Ag/AgCl for the ferri-/ferrocyanide redox couple.[40] Each individual peak's current corresponds to the electrolysis of ferricyanide to ferrocyanide in one water droplet. Upon the collision of the droplet, if the electrode is biased sufficiently to promote the electron transfer from the metal to the species in the droplet, an increase in the cathodic current should be observed. This increase in current is due to the electrolysis of the species in the droplet and when species are available to be reduced, the current returns to baseline. Comparing amperometric *i-t* curves in the presence of $LiClO_4$ (**Figure 3a**) and the presence of TBAP (**Figure 3b**) we can observe individual collisions of water droplets, demonstrating that similar data may be obtained from the two systems. By decreasing the surface area from 28 μm^2 to 0.49 nm^2, collisions are observed displaying that electron transfer across the electrode-water interface is not impeded with the addition of supporting electrolyte in the water droplets and not in the 1,2-dichloroethane phase.

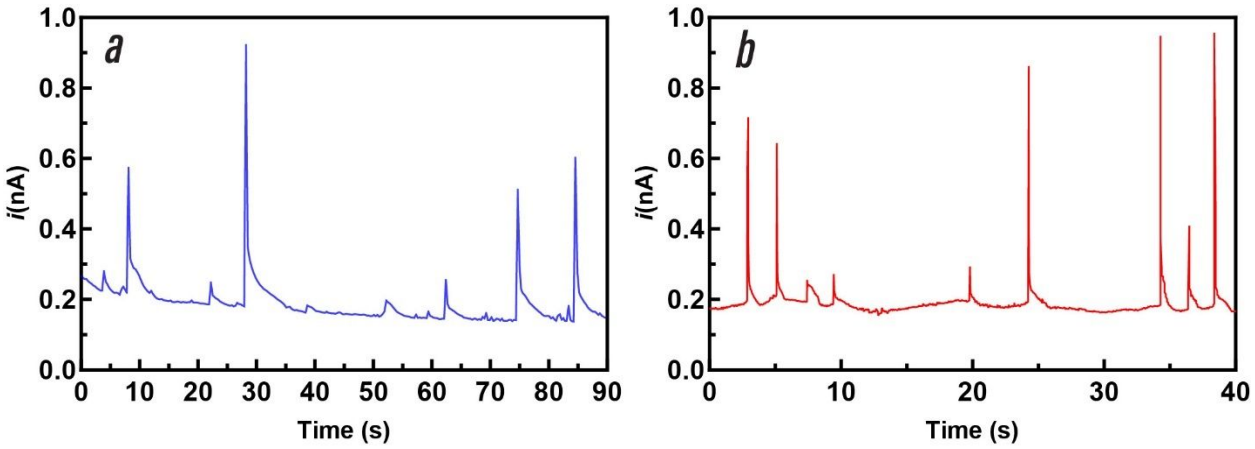

Figure 4. Representative amperometric *i-t* curves of water droplets containing 50 mM hexachloroplatinic acid in the water droplets using an Au UME are shown at a biased potential of -0.3 V vs Ag/AgCl. The first solution contained **a)** 50 mM hexachloroplatinic acid with 250 mM $LiClO_4$ in water droplets suspended in 1,2-dichloroethane, while the second solution contained **b)** 50 mM hexachloroplatinic acid in water droplets suspended in 1,2-dichloroethane with 0.1 M TBAP. The average droplet radius for the system with $LiClO_4$ and TBAP is 1169 nm ± 401 nm (N=16) and 776 nm ±189 nm (N=13) respectively. The potential was selected based on the reduction potential of hexachloroplatinic acid. Droplet sizes were calculated using **Equation 1. TBAP= tetrabutylammonium perchlorate**

To further probe the system with the addition of supporting electrolyte in the water droplets (i.e., $LiClO_4$) and not in the 1,2-dichloroethane phase, we show amperometric *i-t* curves of the electrodeposition of Pt on an Au UME with either $LiClO_4$ in the water droplets (**Figure 4a**) or TBAP in the 1,2-dichloroethane (**Figure 4b**) serving as the supporting electrolyte. The individual collisions presented are the electrolysis of hexachloroplatinic acid species in a single droplet (**Figure 4**),[24] exhibiting that both setups provide similar data. Further, both setups provided the same order of magnitude for the measured current, indicating that the new system, containing $LiClO_4$ as the supporting electrolyte, can be used to perform amperometric *i-t* curve studies. The increase in current displays that $PtCl_6^{2-}$ is being reduced to form Pt^0. When no more species are available to consume, there is an exponential decay in the current returning to baseline.

So far it has been demonstrated that nanoparticles can be obtained electrochemically while using only a small amount of supporting electrolyte in the water droplets. Additionally, another advantage of using the system with $LiClO_4$ is the cost per experiment. For every 5 mL of the 1,2 dichloroethane, 0.17 grams of TBAP were needed to prepare the water-in-oil emulsion with 0.1 M TBAP. A 50-gram TBAP container from Sigma Aldrich has a price of $248; to use all 50 grams, 292 emulsions (5 mL each) could be prepared. However, having supporting electrolyte solely in

the water phase, such as $LiClO_4$, the mass needed is much less leading to a significant price differential. A 100-gram container of battery-grade $LiClO_4$ costs around $329 from Sigma Aldrich. The amount needed to obtain a concentration of 250 mM in 25 μL of water was 6.7×10^{-4} grams; to consume 100 grams (added in 25 μL of the water phase), 150,376 emulsions could be prepared. Each experiment that uses TBAP would cost $1.7, while each experiment with $LiClO_4$ would cost $0.0020. This drives down the experimental cost by a factor of 850. Moreover, we assume for the calculations that the supporting electrolytes, TBAP and $LiClO_4$, cannot be recovered after the reduction of platinum since these substrates are cleaned after the electrodeposition process. See **Table 1** for summarized information about the cost.

Table 1. Summarize of cost while preparing a water-in-oil emulsion with 25 μL of the water phase suspended in 5 mL of the 1,2-dichloroethane phase.

Reagents	Price of the reagents in dollars (100 grams)	Number of emulsions to consume 100 grams	Amount in grams per experiment	Price per experiment in dollars
$LiClO_4$	329	150,376	6.7×10^{-4}	0.0020
TBAP	496	584	0.17	1.7

Conclusions

Nanodroplet-mediated electrodeposition has shown to be a promising technique to synthesize ligand-free nanoparticles. In this paper, we established the advantages of electrodepositing nanoparticles in the presence of supporting electrolyte (*i.e.,* $LiClO_4$) in the water phase only. Amperometric *i-t* curves served as evidence of electron transfer across the metal-water interface even with a highly resistive 1,2-dichloroethane solution. The supporting electrolyte, $LiClO_4$ in the water phase, facilitates the electron transfer across the metal-water interface allowing us to observe amperometric collisions and nanoparticles. This system not only exhibits that we can tune the ion transfer to facilitate the nanoparticle formation but represents a cheaper alternative compared to the addition of the supporting electrolyte (*i.e.,* TBAP) in the 1,2-dichloroethane phase, as the cost is reduced by a factor of 850 per experiment. This is a promising method for different applications such as electrocatalysis, and more, that will serve to help the scientific community and the people in the world for future energy systems.

Author Contributions

All authors have given approval to the final version of the manuscript.

Conflicts of Interest

There are no conflicts to declare.

Acknowledgments

This material is based upon work solely supported as part of the Center for Hybrid Approaches in Solar Energy to Liquid Fuels (CHASE), an Energy Innovation Hub funded by the U.S. Department of Energy, Office of Science, Office of Basic Energy Sciences under Award Number DE-SC0021173. We acknowledge use of scanning electron microscopy and energy dispersive X-ray spectroscopy instrumentation at the Chapel Hill Analytical and Nanofabrication Laboratory, CHANL, a member of the North Carolina Research Triangle Nanotechnology Network, RTNN, which is supported by the National Science Foundation, Grant ECCS-2025064, as part of the National Nanotechnology Coordinated Infrastructure, NNCI.

References

1. Maheshwari, K.; Sharma, S.; Sharma, A.; Verma, S., Fuel Cell and Its Applications: A Review. **2018,** *7* (06).
2. Berg, P.; Novruzi, A.; Volkov, O., Reaction Kinetics at the Triple-Phase Boundary in PEM Fuel Cells. *Journal of Fuel Cell Science and Technology* **2008,** *5* (2).
3. Nitta, N.; Wu, F.; Lee, J. T.; Yushin, G., Li-ion battery materials: present and future. *Materials Today* **2015,** *18* (5), 252-264.
4. Sharma, S.; Kumar Jain, K.; Sharma, A., Solar Cells: In Research and Applications—A Review. **2015,** *6*, 1145-1155.
5. Stevens, M. B.; Kreider, M. E.; Patel, A. M.; Wang, Z.; Liu, Y.; Gibbons, B. M.; Statt, M. J.; Ievlev, A. V.; Sinclair, R.; Mehta, A.; Davis, R. C.; Nørskov, J. K.; Gallo, A.; King, L. A.; Jaramillo, T. F., Identifying and Tuning the In Situ Oxygen-Rich Surface of Molybdenum Nitride Electrocatalysts for Oxygen Reduction. *ACS Applied Energy Materials* **2020,** *3* (12), 12433-12446.
6. Chen, G.; Stevens, M. B.; Liu, Y.; King, L. A.; Park, J.; Kim, T. R.; Sinclair, R.; Jaramillo, T. F.; Bao, Z., Nanosized Zirconium Porphyrinic Metal–Organic Frameworks that Catalyze the Oxygen Reduction Reaction in Acid. *Small Methods* **2020,** *4* (10), 2000085.
7. Gallo, A.; Snider, J. L.; Sokaras, D.; Nordlund, D.; Kroll, T.; Ogasawara, H.; Kovarik, L.; Duyar, M. S.; Jaramillo, T. F., Ni5Ga3 catalysts for CO2 reduction to methanol: Exploring the role of Ga surface oxidation/reduction on catalytic activity. *Applied Catalysis B: Environmental* **2020,** *267*, 118369.

8. Ben-Naim, M.; Palm, D. W.; Strickler, A. L.; Nielander, A. C.; Sanchez, J.; King, L. A.; Higgins, D. C.; Jaramillo, T. F., A Spin Coating Method To Deposit Iridium-Based Catalysts onto Silicon for Water Oxidation Photoanodes. *ACS Applied Materials & Interfaces* **2020,** *12* (5), 5901-5908.
9. Ding, L.-X.; Wang, A.-L.; Li, G.-R.; Liu, Z.-Q.; Zhao, W.-X.; Su, C.-Y.; Tong, Y.-X., Porous Pt-Ni-P Composite Nanotube Arrays: Highly Electroactive and Durable Catalysts for Methanol Electrooxidation. *Journal of the American Chemical Society* **2012,** *134* (13), 5730-5733.
10. Wang, A.-L.; Xu, H.; Feng, J.-X.; Ding, L.-X.; Tong, Y.-X.; Li, G.-R., Design of Pd/PANI/Pd Sandwich-Structured Nanotube Array Catalysts with Special Shape Effects and Synergistic Effects for Ethanol Electrooxidation. *Journal of the American Chemical Society* **2013,** *135* (29), 10703-10709.
11. Wang, A.-L.; He, X.-J.; Lu, X.-F.; Xu, H.; Tong, Y.-X.; Li, G.-R., Palladium–Cobalt Nanotube Arrays Supported on Carbon Fiber Cloth as High-Performance Flexible Electrocatalysts for Ethanol Oxidation. *Angewandte Chemie International Edition* **2015,** *54* (12), 3669-3673.
12. Seetharaman, S.; McLean, A.; L., G. R. I.; Sridhar; S., *Treatise*

on process metallurgy. Elsevier: Oxford: 2014.
13. Chen, D.-H.; Wu, S.-H., Synthesis of Nickel Nanoparticles in Water-in-Oil Microemulsions. *Chemistry of Materials* **2000,** *12* (5), 1354-1360.
14. Lei, B.; Xue, J.; Jin, D.; Ni, S.; Sun, H., Fabrication, annealing, and electrocatalytic properties of platinum nanoparticles supported on self-organized TiO2 nanotubes. *Rare Metals* **2008,** *27* (5), 445-450.
15. Cunci, L.; Velez, C. A.; Perez, I.; Suleiman, A.; Larios, E.; José-Yacamán, M.; Watkins, J. J.; Cabrera, C. R., Platinum Electrodeposition at Unsupported Electrochemically Reduced Nanographene Oxide for Enhanced Ammonia Oxidation. *ACS Applied Materials & Interfaces* **2014,** *6* (3), 2137-2145.
16. Cao, S.; Tao, F.; Tang, Y.; Li, Y.; Yu, J., Size- and shape-dependent catalytic performances of oxidation and reduction reactions on nanocatalysts. *Chemical Society Reviews* **2016,** *45* (17), 4747-4765.
17. Wuithschick, M.; Paul, B.; Bienert, R.; Sarfraz, A.; Vainio, U.; Sztucki, M.; Kraehnert, R.; Strasser, P.; Rademann, K.; Emmerling, F.; Polte, J., Size-Controlled Synthesis of Colloidal Silver Nanoparticles Based on Mechanistic Understanding. *Chemistry of Materials* **2013,** *25* (23), 4679-4689.
18. Kunz, S., Supported, Ligand-Functionalized Nanoparticles: An Attempt to Rationalize the Application and Potential of Ligands in Heterogeneous Catalysis. *Topics in Catalysis* **2016,** *59* (19), 1671-1685.
19. Kauffman, D. R.; Ohodnicki, P. R.; Kail, B. W.; Matranga, C., Selective Electrocatalytic Activity of Ligand Stabilized Copper Oxide Nanoparticles. *The Journal of Physical Chemistry Letters* **2011,** *2* (16), 2038-2043.
20. Fan, X.; Zerebecki, S.; Du, R.; Hübner, R.; Marzum, G.; Jiang, G.; Hu, Y.; Barcikowki, S.; Reichenberger, S.; Eychmüller, A., Promoting the Electrocatalytic Performance of Noble Metal Aerogels by Ligand-Directed Modulation. *Angewandte Chemie International Edition* **2020,** *59* (14), 5706-5711.
21. Ernst, A. Z.; Sun, L.; Wiaderek, K.; Kolary, A.; Zoladek, S.; Kulesza, P. J.; Cox, J. A., Synthesis of Polyoxometalate-Protected Gold Nanoparticles by a Ligand-Exchange Method: Application to the Electrocatalytic Reduction of Bromate. *Electroanalysis* **2007,** *19* (19-20), 2103-2109.
22. Walker, N. L.; Roshkolaeva, A. B.; Chapoval, A. I.; Dick, J. E., Recent advances in potentiometric biosensing. *Current Opinion in Electrochemistry* **2021,** *28*, 100735.
23. Zhang, H.; Sepunaru, L.; Sokolov, S. V.; Laborda, E.; Batchelor-McAuley, C.; Compton, R. G., Electrochemistry of single droplets of inverse (water-in-oil) emulsions. *Physical Chemistry Chemical Physics* **2017,** *19* (24), 15662-15666.
24. Glasscott, M. W.; Dick, J. E., Direct Electrochemical Observation of Single Platinum Cluster Electrocatalysis on Ultramicroelectrodes. *Analytical Chemistry* **2018,** *90* (13), 7804-7808.
25. Tasakorn, P.; Chen, J.; Aoki, K., Voltammetry of a single oil droplet on a large electrode. *Journal of Electroanalytical Chemistry* **2002,** *533* (1), 119-126.

26. Aoki, K.; Tasakorn, P.; Chen, J., Electrode reactions at sub-micron oil|water|electrode interfaces. *Journal of Electroanalytical Chemistry* **2003,** *542*, 51-60.
27. Kim, B.-K.; Kim, J.; Bard, A. J., Electrochemistry of a Single Attoliter Emulsion Droplet in Collisions. *Journal of the American Chemical Society* **2015,** *137* (6), 2343-2349.
28. Terry Weatherly, C. K.; Ren, H.; Edwards, M. A.; Wang, L.; White, H. S., Coupled Electron- and Phase-Transfer Reactions at a Three-Phase Interface. *Journal of the American Chemical Society* **2019,** *141* (45), 18091-18098.
29. Glasscott, M. W.; Pendergast, A. D.; Dick, J. E., A Universal Platform for the Electrodeposition of Ligand-Free Metal Nanoparticles from a Water-in-Oil Emulsion System. *ACS Applied Nano Materials* **2018,** *1* (10), 5702-5711.
30. Jeun, Y. E.; Park, J. H.; Kim, J. Y.; Ahn, H. S., Stoichiometry-Controlled Synthesis of Nanoparticulate Mixed-Metal Oxyhydroxide Oxygen Evolving Catalysts by Electrochemistry in Aqueous Nanodroplets. *Chemistry – A European Journal* **2020,** *26* (18), 4039-4043.
31. Jeun, Y. E.; Baek, B.; Lee, M. W.; Ahn, H. S., Surfactant-free electrochemical synthesis of metallic nanoparticles via stochastic collisions of aqueous nanodroplet reactors. *Chemical Communications* **2018,** *54* (72), 10052-10055.
32. Lee, M. W.; Kwon, D.-J.; Park, J.; Pyun, J.-C.; Kim, Y.-J.; Ahn, H. S., Electropolymerization in a confined nanospace: synthesis of PEDOT nanoparticles in emulsion droplet reactors. *Chemical Communications* **2020,** *56* (67), 9624-9627.
33. Glasscott, M. W.; Hill, C. M.; Dick, J. E., Quantifying Growth Kinetics of Single Nanoparticles in Sub-Femtoliter Reactors. *The Journal of Physical Chemistry C* **2020,** *124* (26), 14380-14389.
34. Glasscott, M. W.; Dick, J. E., Fine-Tuning Porosity and Time-Resolved Observation of the Nucleation and Growth of Single Platinum Nanoparticles. *ACS Nano* **2019,** *13* (4), 4572-4581.
35. Terry Weatherly, C. K.; Glasscott, M. W.; Dick, J. E., Voltammetric Analysis of Redox Reactions and Ion Transfer in Water Microdroplets. *Langmuir* **2020,** *36* (28), 8231-8239.
36. Glasscott, M. W.; Voci, S.; Kauffmann, P. J.; Chapoval, A. I.; Dick, J. E., Mapping Solvent Entrapment in Multiphase Systems by Electrogenerated Chemiluminescence. *Langmuir* **2021,** *37* (9), 2907-2912.
37. Glasscott, M. W.; Dick, J. E., Visualizing Phase Boundaries with Electrogenerated Chemiluminescence. *The Journal of Physical Chemistry Letters* **2020,** *11* (12), 4803-4808.
38. Sabaragamuwe, S. G.; Conti, D.; Puri, S. R.; Andreu, I.; Kim, J., Single-Entity Electrochemistry of Nanoemulsion: The Nanostructural Effect on Its Electrochemical Behavior. *Analytical Chemistry* **2019,** *91* (15), 9599-9607.
39. Vannoy, K. J.; Ryabykh, A.; Chapoval, A. I.; Dick, J. E., Single enzyme electroanalysis. *Analyst* **2021,** *146* (11), 3413-3421.
40. Bard, A. J. F., Larry R., *Electrochemical Methods: Fundamentals and Applications*. 2nd edition ed.; John Wiley & Sons: New York, 2001.
41. Deng, H.; Dick, J. E.; Kummer, S.; Kragl, U.; Strauss, S. H.; Bard, A. J., Probing Ion Transfer across Liquid–Liquid Interfaces by Monitoring Collisions of Single Femtoliter Oil Droplets on Ultramicroelectrodes. *Analytical Chemistry* **2016,** *88* (15), 7754-7761.
42. Osakai, T.; Naito, Y.; Eda, K.; Yamamoto, M., Prediction of the Standard Gibbs Energy of Transfer of Organic Ions Across the Interface between Two Immiscible Liquids. *The Journal of Physical Chemistry B* **2015,** *119* (41), 13167-13176.
43. Walsh, F. C.; Herron, M. E., Electrocrystallization and electrochemical control of crystal growth: fundamental considerations and electrodeposition of metals. *Journal of Physics D: Applied Physics* **1991,** *24* (2), 217-225.

44. Abyaneh, M. Y.; Fleischmann, M.; Del Giudice, E.; Vitiello, G., The investigation of nucleation using microelectrodes: I. The ensemble averages of the times of birth of the first nucleus. *Electrochimica Acta* **2009,** *54* (3), 879-887.